

## Capping Rigid Origami Tubes

Tomohiro TACHI\*

\* The University of Tokyo  
3-8-1 Komaba, Meguro-Ku, Tokyo 153-8902, Japan  
tachi@idea.c.u-tokyo.ac.jp

### Abstract

Origami-based deployable systems that encloses a volume can be actuated through pneumatics or hydraulics. The potential applications include deployment of spatial structures and metamaterials that can be tuned by pressures. Rigid origami tubes and their assembly can form such a transformable and tunable material, but the end design to cap the tubular system making into a closed system has been an unsolved issue. In fact, this issue is mathematically proved to be unsolvable by the Bellows theorem, which says that a closed polyhedron cannot change its volume when each facet keeps isometry.

We find an engineering way-around to this problem to produce a close-to-rigid-foldable cap designs for rigid foldable tubes. Specifically, we introduce a parametric design of infinitesimally rigid foldable structures and multi-stable structures that can fit to a transformable planar parallelogram section. This structure can be attached to the ends of a rigid foldable origami tube to cap them. The proposed structure can act as a component to build bellows or hydraulic actuators, as well as the method for creating a compliant covering of scissors mechanisms.

**Keywords:** origami, bellows, rigidity, structural morphology

### 1 Bellows do not exist.

**Introduction** A motivation for applying the concept of origami, i.e, surface folding, to deployable and transformable systems comes from the fact that origami concepts can lead to both a kinematic system that folds compactly and a spatial structure with watertight surface. In the ultimate, it is natural to expect that origami can be used for realizing both, i.e., a closed volume with kinematic flat-folding. If such a structure is realized, we may produce perfect bellows, pneumatic and hydraulic actuators, foldable containers, temporary shelters, habitation modules of a space station, and so on.

We consider an approach toward realizing such structures by "capping" tubular origami structures [9]. The tubular origami structures are known to be rigid-foldable, meaning that a kinematic motion is obtained even if each panel is kept rigid. If we are able to cap these rigid-foldable tubes with a mechanism with watertight surface, we can make a bellows where its volume change is controlled by its lengths; or a pneumatic actuator where the volume change triggers the expanding motion along the axis. One of many advantages of the system is that the folded state is extremely compact compared to the existing

piston actuators.

So, does such a “rigid-foldable bellows” exist? The theoretical answer is NO; according to the Bellows theorem [4], a closed polyhedron cannot change its volume continuously. Flexible polyhedra exist [3] but cannot be collapsed to zero volume or otherwise it is self-intersecting [2]. This is why the capping of origami tube remains to be an unsolved problem [8].

**Way-around Ideas** There are potentially several way-around approaches toward this problem. One hack is to add a tiny slit or hole to the closed polyhedron, so that it is no longer a closed polyhedron. For example, a tetrahedron can be flattened by rigid folding motion by adding a slit of 4.6% of its edge length [1]. Another way-around is to use the compliance of the panel against in-plane deformation. In this case, the strain energy is stored during the folding motion, and typically released at some discrete positions, making the system multi-stable structure [6, 7].

This paper explores a family of a cap design based on the latter approach of allowing for a small stretch of panels during its motion. By the choice of design parameters, we may form tristable structures, bistable structures with an infinitesimal flexibility, and monostable structures with second-order flexibility. Figure 1 shows a second-order flexible cap attached to a rigid foldable cylinder.



Figure 1: An example capped tube with second-order flexibility.

## 2 Basic Geometry

### 2.1 The deformation of tube’s section

We consider the basic rigid foldable tube [9], composed by mirroring a Miura-ori sheet (Figure 2). Here, the boundary shape is a (planar) rhombus that shears as the tube folds. Specifically, for a tube composed of parallelogram faces of angle  $\theta$ , the half of the sector angle  $\varphi$  of the boundary rhombus change as

$$\sin \varphi(s) = s \sin \theta \quad (1)$$

where  $s = \sin \frac{\rho}{2}$  is the sine of half of the fold angle  $\rho$  between adjacent panels. As  $s$  moves  $0 \rightarrow 1$ ,  $\varphi(s)$  changes  $0 \rightarrow \theta$ .

Here, the deployed length of the tube changes proportionally to  $\sin \xi$ , where  $\xi$  is the angle of section plane and the tube’s extrusion direction. By solving the isometry constraints given by

$$\cos \xi(s) \cos \varphi(s) = \cos \theta, \quad (2)$$

we get,

$$z(s) = z(0) \sqrt{1 - \frac{\cos^2 \theta}{1 - s^2 \sin^2 \theta}} \quad (3)$$

### 2.2 Design Parameters

**Antiprism Cap** The target cap is a polyhedral surface whose boundary is a rhombus, and it deforms in a way that the out-of-plane motion of the section is small enough and thus the boundary is almost

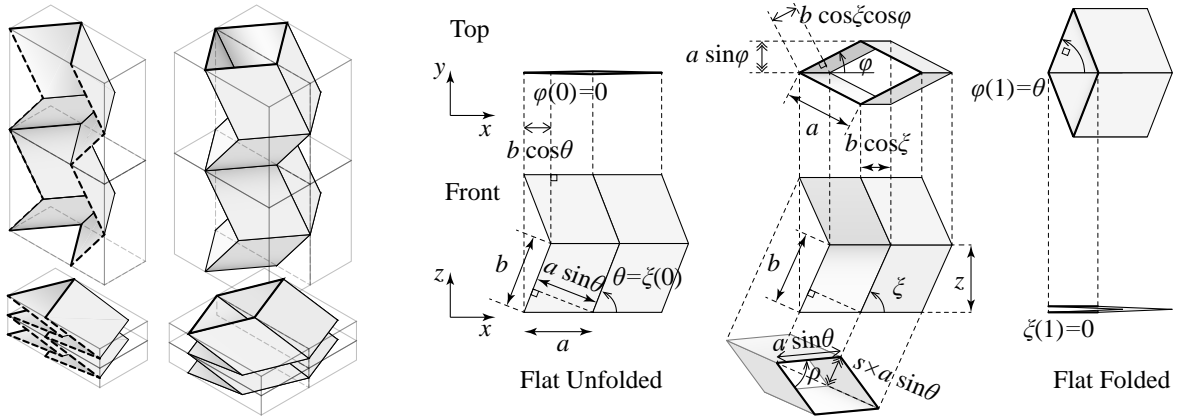


Figure 2: Rigid-foldable tube.

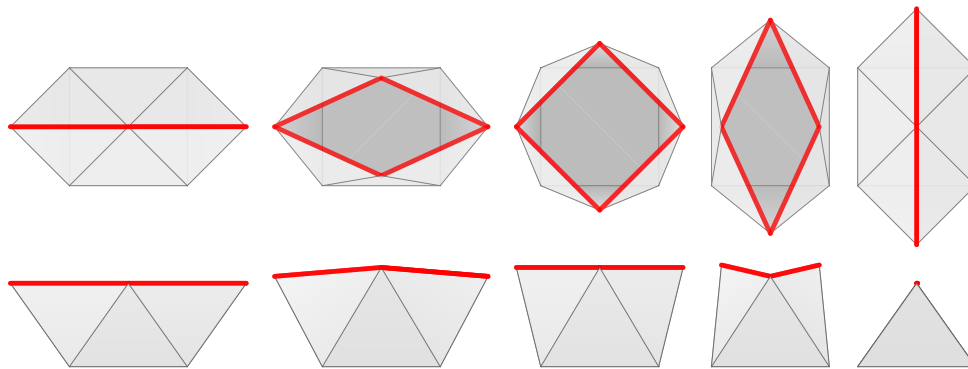


Figure 3: Rigid folding motion of a regular antiprism cap.

rhombus during the folding motion. We start a design exploration from the polyhedral surface formed by removing the top base face of a quadrangular antiprism. A particular design based on regular antiprism is shown in Figure 3; this has three states where the boundary lies within a plane, and thus can form a tri-stable system when we force the planarity of the boundary. We explore the design variations from this basic concept to produce systems with different stability.

**Model** To explore the design of a near-flexible system and its “kinematics”, we consider a “partially rigid origami model.” In this model, we assume some set of constraints to be active and thus forming one-DOF mechanism, and the remaining set of constraints are free, but we measure its error, and use them to measure the difference from an ideal kinematic system. In the quasi-static process of an actual elastic model, each panel deforms simultaneously such that the total strain energy is minimized; therefore, the partially rigid origami model can give an upper bound of the strain energy in the actual elastic model<sup>1</sup>, so it is an easy model for understanding the behavior of the system.

For the convenience, we employ the following parameterization (See Figure 4). We place the center of the tube on the  $z$  axis. A cap consists of

1. *base rectangle* with  $x$  and  $y$  dimensions being  $2a$  and  $2b$ , respectively, remaining rigid in place;
2. two pairs of *wall triangles* attached to the lateral and longitudinal edges (of edge lengths  $2a$  and  $2b$ , respectively) of the bottom rectangle, remaining rigid, i.e., the heights  $q$  and  $p$  of the lateral

<sup>1</sup>Inappropriate choice of parameters may result in an overestimation of rigidity in general, but underestimation does not happen

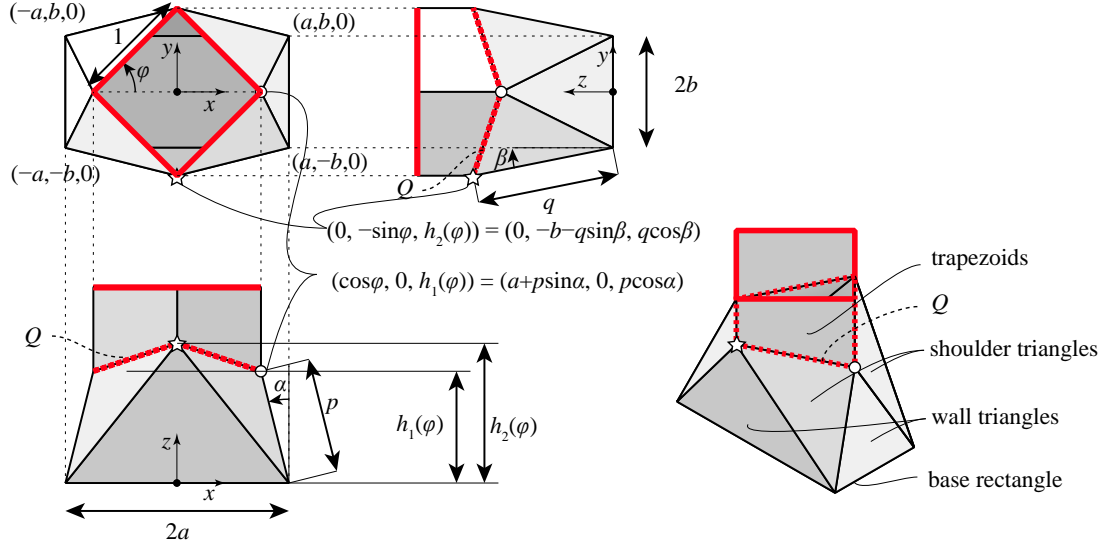


Figure 4: Notations for cap design.

- and longitudinal wall triangles along the panels, respectively, are unchanged;
3. four identical *shoulder triangles* that connect the sides of wall triangles, whose base edges form a quadrangle  $Q$  (the planar boundary of the example in Figure 3 is  $Q$ ), freely deformable; and
  4. in addition, to allow for more generalized designs, a cylinder formed by four vertical trapezoids attached to  $Q$  to form a planar rhombic boundary (assuming the edge length to be 1); whose projection to  $z$  direction is unchanged.

With this assumption, the deformation of every shoulder triangle is restricted by the deformation of surrounding faces, so the deformation of remaining constraints can be expressed as the vertical stretch of trapezoids caused by the non-equal vertical motions of the apices of wall triangles. Therefore, we measure *the change in  $z$  dimension of  $Q$*  as the error from the (non-existent) ideal kinematic cap.

### 2.3 Error Evaluation

The kinematics can be expressed as follows: let  $\alpha$  and  $\beta$  the rotation angles of lateral and longitudinal wall triangles with respect to vertical (parallel to  $z$  direction), respectively. Then the coordinates of corners of  $Q$  can be represented as  $(\pm(a + p \sin \alpha), 0, p \cos \alpha)$  and  $(0, \pm(b + q \sin \beta), q \cos \beta)$ .  $Q$  must be projected to rhombus with unit length edges in  $xy$  plane, so

$$\cos \varphi = a + p \sin \alpha \quad (4)$$

$$\sin \varphi = b + q \sin \beta, \quad (5)$$

where  $\varphi$  is the angle of the section rhombus (the same parameter  $\varphi$  of the tube's rhombus).

Therefore, the heights  $h_1(\varphi)$  and  $h_2(\varphi)$  of corners of  $Q$  are represented as

$$h_1(\varphi) := p \cos \alpha = \sqrt{p^2 - (\cos \varphi - a)^2} \quad (6)$$

$$h_2(\varphi) := q \cos \beta = \sqrt{q^2 - (\sin \varphi - b)^2} \quad (7)$$

So, we want to keep the  $z$  dimension  $h(\varphi)$  of  $Q$

$$h(\varphi) := h_1(\varphi) - h_2(\varphi) \quad (8)$$

as constant as possible, or in other words, keep  $e(\varphi) = h(\varphi) - h_0$  as close to 0 as possible. We characterize this by looking at the solution space of  $e(\varphi) = 0$  in  $0 < \varphi < \frac{\pi}{2}$  (or  $0 < \varphi < \theta$  when attached to a foldable tube of sector angle  $\theta$ ).

Notice that  $e(\varphi)$  is related to the strain of the trapezoids at the boundary. If we assume that the strain  $\varepsilon$  is constant over the panel,  $\varepsilon \propto e(\varphi)$ . Therefore, for an elastic system, we can evaluate the strain energy by  $U(\varphi) = \frac{1}{2}e(\varphi)^2$  (multiplied by some constant factor), and thus the angular stiffness of the section rhombus by  $K(\varphi) = \left(\frac{de}{d\varphi}\right)^2 + e(\varphi)\frac{d^2e(\varphi)}{d\varphi^2}$ .

### 3 Solution

#### 3.1 Observation

In this paper, we first consider a special case where the trapezoids composing the top tube are rectangles and thus  $h_0 = 0$ . Then the solution of  $e(\varphi) = h(\varphi) = 0$  in  $\varphi \in [0^\circ, 90^\circ]$  is given by the intersection between (1) a hyperbola  $-x^2 + y^2 + (p^2 - q^2) = 0$  restricted to  $(x, y) \in [-p, p] \times [-q, q]$  and (2) the arc of a quarter circle  $(x, y) = (\cos \varphi - a, \sin \varphi - b)$  for  $\varphi \in [0^\circ, 90^\circ]$ . Figure 5 shows the plots of these curves for different parameters. When the cap's vertical projection is equal to a regular antiprism, i.e., the cap with  $a = b = \frac{1}{2}$  and  $p = q$  the intersection of curves will give three solutions at  $\varphi = 0, 45^\circ, 90^\circ$ . The three configurations get close to each other when we move the arc centers away by increasing  $a$  and  $b$ . This will eventually cause the merge of three solutions into one triple root at  $\varphi = 45^\circ$  with the critical parameter of  $a = b = \frac{1}{\sqrt{2}}$  and  $p = q$  (Figure 5 (b) and Figure 1). At such a point, the system becomes mono-stable but with zero-stiffness; more precisely, from the viewpoint of rigidity, the structure is second-order flexible at the configuration (see Section 4 for the flexibility). If we pass the critical position, the system becomes monostable and first-order rigid (Figure 5 (c)).

#### 3.2 Design from 3 positions

In general, we may solve the design parameters by specifying 3 angles  $\varphi = \varphi_1, \varphi_2, \varphi_3$  where the intersection lies as:

$$a = \frac{1}{2}(\cos(\varphi_1 + \varphi_2 + \varphi_3) + \cos \varphi_1 + \cos \varphi_2 + \cos \varphi_3) \quad (9)$$

$$b = \frac{1}{2}(-\sin(\varphi_1 + \varphi_2 + \varphi_3) + \sin \varphi_1 + \sin \varphi_2 + \sin \varphi_3) \quad (10)$$

$$p^2 - q^2 = \cos(\varphi_1 + \varphi_2) \cos(\varphi_2 + \varphi_3) \cos(\varphi_3 + \varphi_1) \quad (11)$$

We may use these solution for tweaking the tube behaves in a desired way. Here are typical designs generated using this method.

1. Provide three angles corresponding to deployed states of the tube in use. For example, we want to cap a tube with  $\theta = 75^\circ$ . Then, we may give  $\varphi_1 = 0^\circ, \varphi_2 = 45^\circ, \varphi_3 = 75^\circ$  to solve the parameters of the cap  $(a, b, p^2 - q^2) = \left(\frac{\sqrt{2}+\sqrt{6}+2}{8}, \frac{3\sqrt{2}-2\sqrt{3}+\sqrt{6}}{8}, \frac{1-\sqrt{3}}{8}\right) \approx (0.404, 0.733, -0.0915)$  as in

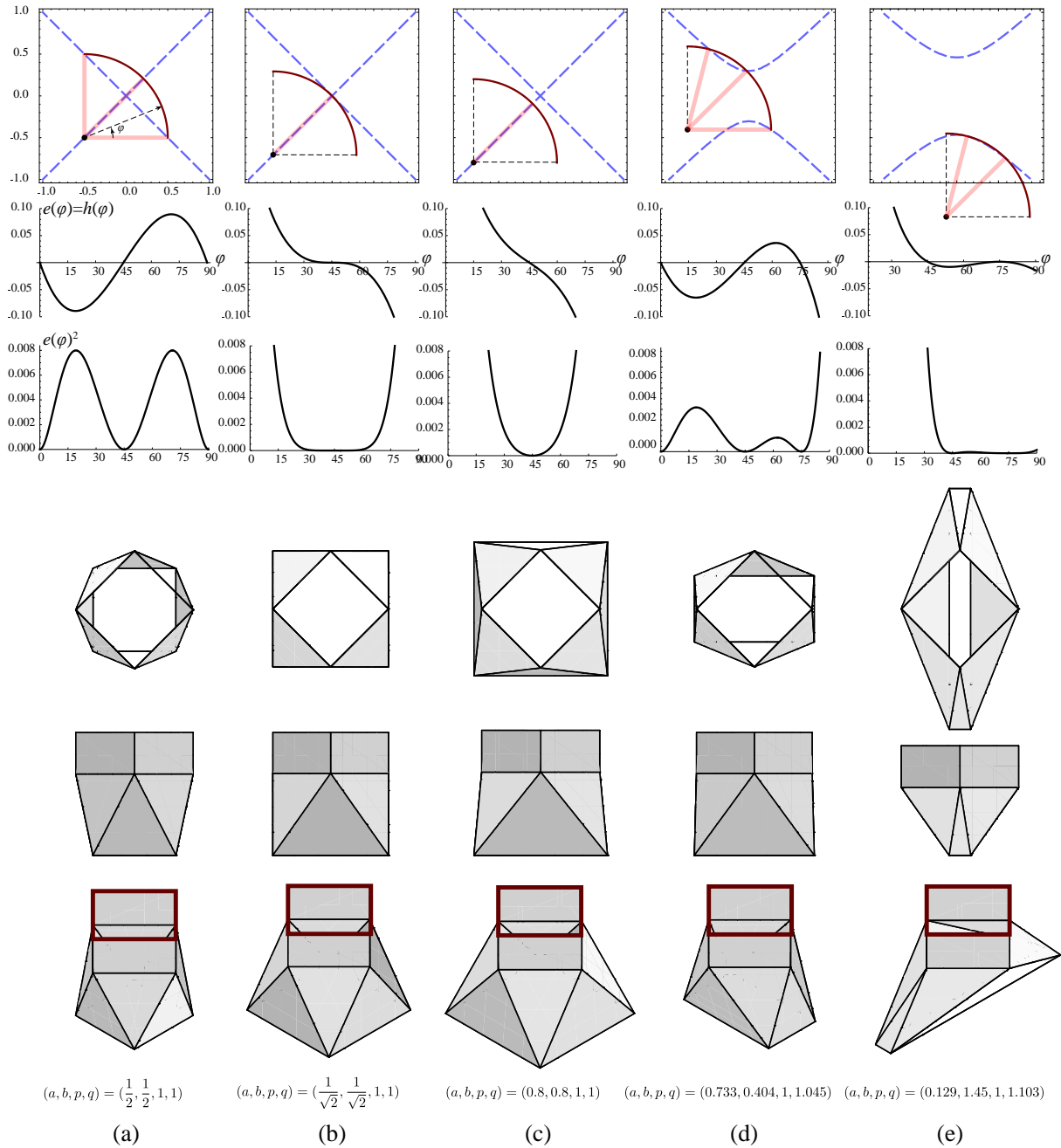


Figure 5: First row: intersections of two curves. Second row: plot of  $e(\varphi) = h(\varphi)$  (proportional to strain). Third row: plot of  $e(\varphi)^2$  (proportional to energy). Fourth to sixth rows: top, front and isometric view of the cap in  $\varphi = 45^\circ$ . (a) regular cap (projection of a regular anti-prism) with 3 stable points. (b) second-order flexible cap with  $p = q$  (c) mono-stable cap with  $p = q$  (d) cap stable at  $\varphi = 15^\circ, 45^\circ, 90^\circ$  (e) cap infinitesimally flexible at  $\varphi = 15^\circ$  and stable at  $45^\circ$

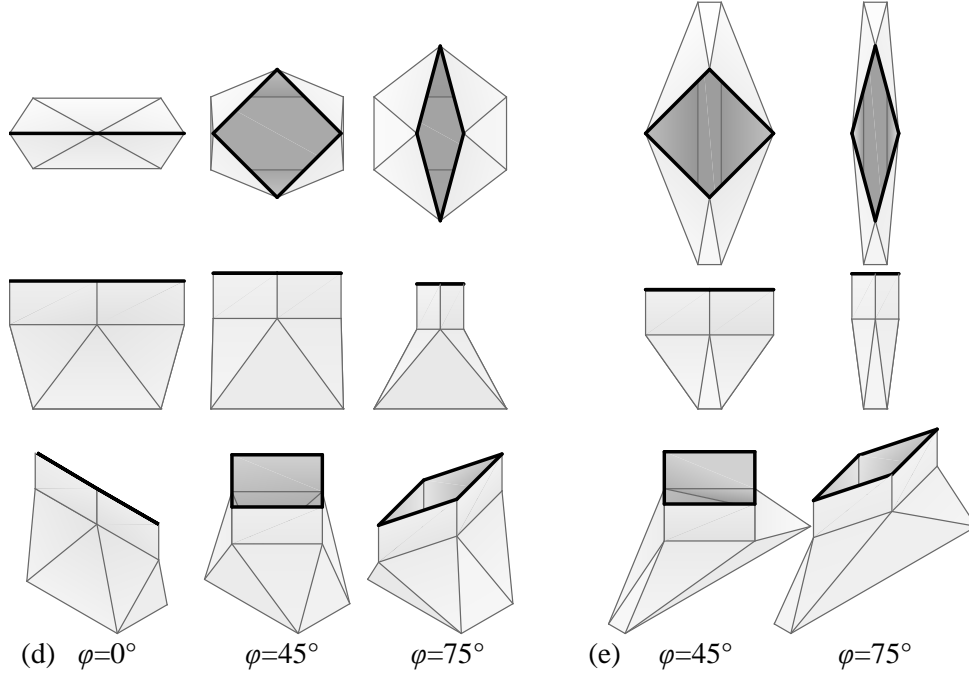


Figure 6: The folded states of tubes (d) and (e).

Figures 5 (d) and 6 (d). This design is compatible with the tube and stable at two extreme flat-positions  $\phi = 0^\circ, 75^\circ$  and at a deployed state  $\phi = 45^\circ$ .

2. Provide double root for one the flat-folded state, and also a root at a deployed state. This is using that in general, the configuration at the double root has infinitesimally flexibility. For example, for a given tube with  $\theta = 75^\circ$ , we give the following roots  $\varphi_1 = 45^\circ, \varphi_2 = 75^\circ, \varphi_3 = 75^\circ$ . This will solve to  $(a, b, p^2 - q^2) = (\frac{\sqrt{2-\sqrt{3}}}{4}, \frac{3\sqrt{2+\sqrt{3}}}{4}, -\frac{\sqrt{3}}{8}) \approx (1.45, 0.129, -0.217)$  as in Figures 5 (e) and 6 (e). This will make the initial deployment phase at  $\varphi_2 = 75^\circ$  first-order flexible, and then snaps to a deployed state of  $\phi = 45^\circ$ .
3. Provide a triple root for one state by giving  $\phi_1 = \phi_2 = \phi_3 = \phi_0$ . For example, Figure 5 (b) shows the case where  $\phi_0 = 45^\circ$ . We may use this structure for the design of bellows and actuators. As described in Section 4, the tube structure with this cap may become a third order flexible with nontrivial first order change in the axial dimension.

### 3.3 Other Design Parameters

In the design above, we fixed  $p = 1$  and  $h = 0$ . By tweaking these parameters, we may obtain slightly more complex behavior.

**Tweaking  $p$**  Equation (11) leaves the possibility to tweak  $p$ , by increasing and decreasing  $p$  together with  $q$ . As  $p$  and  $q$  are the height of wall triangles along the panel, if they are big enough, the amount of change in  $\alpha$  and  $\beta$  to fit the given deformation of section rhombus gets smaller (see Figure 4). As a result, for a structure satisfying (9)–(11),  $e$  decreases when  $p$  and  $q$  increase; in the extreme, if  $p, q \rightarrow \infty$ , then non-linear term of  $h_1$  and  $h_2$  will disappear, and thus  $e \rightarrow 0$ . On the other hand, if  $p$  and  $q$  are small, there the rotation of wall triangle according to  $\phi$  becomes bigger and  $e$  gets larger. At an extreme, if  $p < |\cos \phi - a|$  or  $p < |\sin \phi - b|$ , then there is no  $\alpha$  or  $\beta$  that satisfies (4) and (5). This can be

used for limiting the folding motion at a certain angle, and to increase the stiffness at the deployed state by increasing  $\frac{\partial e}{\partial \phi}$ . For example, the model in Figure 7 right uses the same parameters  $a, b, p^2 - q^2$  as in Figure 5 (e) (Figure 7 left), but uses  $p = 0.58, q = 0.744$  instead of  $p = 1, q = 1.103$ . Notice that this structure gets “locked” at the deployed state of  $\phi = 45^\circ$ .

The calculated stiffness can unrealistically approach infinity in our model. The overestimated stiffness is the artifact caused by the assumption that triangular walls and bottom rectangles are rigid, i.e., infinitely stiff. In reality, the wall triangles and the bottom rectangle are expected to deform more as the value of  $\frac{\partial e}{\partial \phi}$  gets larger in our model.

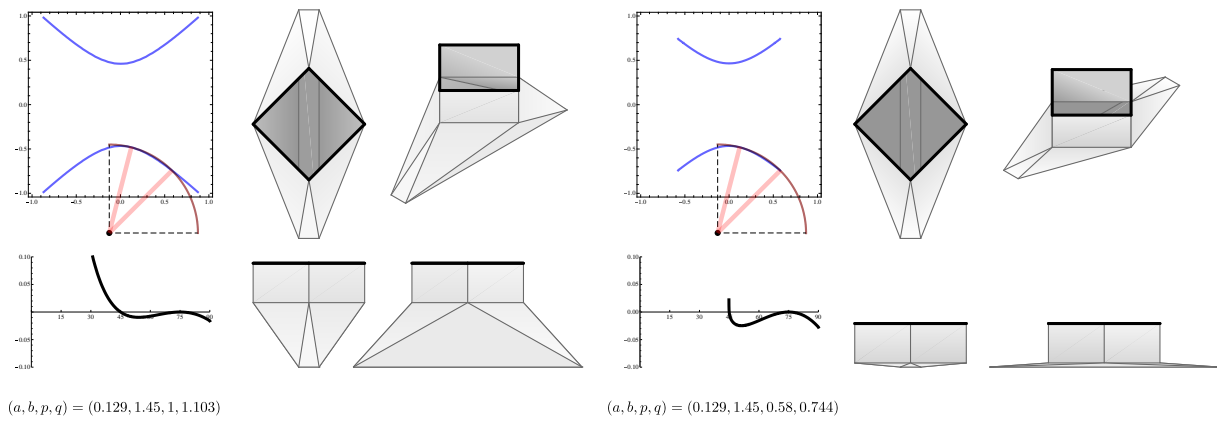


Figure 7: A tube that can be locked at the deployed state (right) with smaller  $p$  than the one on left.

**Tweaking  $h$**  Allowing for  $h \neq 0$  potentially provides 4 or more solutions to  $h(\phi) = h$ ; however, we were not able to obtain simple closed forms as in (9)–(11). Figure 8 shows an example design with four solutions. The effect of parameter  $h$  in the overall behavior of the tube remains not explored in this study.

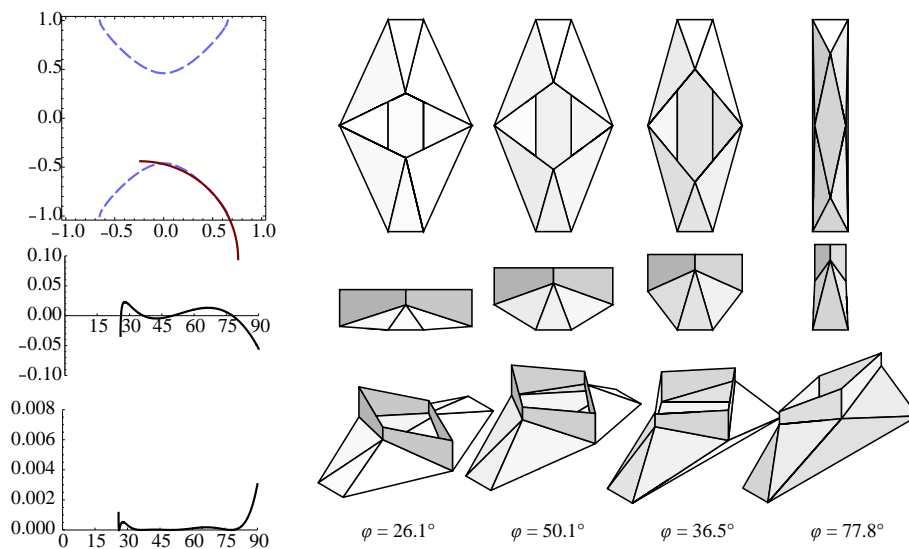


Figure 8: A tube with  $a = 0.24, b = 1.44, p = 0.66, q = 1.056, h = -0.29$  having four stable configurations at  $\phi = 26.1^\circ, 50.1^\circ, 36.5^\circ, 77.8^\circ$ .

## 4 Flexibility

When we have a triple root, the system becomes second-order flexible at the configuration. Figure 9 shows the second order flex  $(\mathbf{x}^{(1)}, \mathbf{x}^{(2)})$  of the structure, where for a set of vertex positions  $\mathbf{x} = [\mathbf{x}_1, \dots, \mathbf{x}_V]^T$  (where  $V = 12$  is the number of vertices),  $\mathbf{x}^{(1)}$  and  $\mathbf{x}^{(2)}$  represent the velocity and acceleration of the vertices, respectively.  $(\mathbf{x}^{(1)}, \mathbf{x}^{(2)})$  is a second order flex if and only if for each edge between  $u$ -th and  $v$ -th vertices ( $1 \leq u, v \leq V$ ) ([5]) satisfies both of

$$(\mathbf{x}_u - \mathbf{x}_v) \cdot (\mathbf{x}_u^{(1)} - \mathbf{x}_v^{(1)}) = 0 \quad (12)$$

$$(\mathbf{x}_u^{(1)} - \mathbf{x}_v^{(1)}) \cdot (\mathbf{x}_u^{(1)} - \mathbf{x}_v^{(1)}) + (\mathbf{x}_u - \mathbf{x}_v) \cdot (\mathbf{x}_u^{(2)} - \mathbf{x}_v^{(2)}) = 0. \quad (13)$$

If there is a second order flex, then the structure is second-order flexible. From Figure 9, we can check vertices  $u, v, w$  and edges between  $(u, v)$ ,  $(u, w)$  and  $(v, w)$  in Figure 9 all satisfy (12) and (13), e.g.,  $(\mathbf{x}_v^{(0)} - \mathbf{x}_w^{(0)}) \cdot (\mathbf{x}_v^{(1)} - \mathbf{x}_w^{(1)}) = 0$ ,  $(\mathbf{x}_v^{(1)} - \mathbf{x}_w^{(1)}) \cdot (\mathbf{x}_v^{(1)} - \mathbf{x}_w^{(1)}) = 1$  and  $(\mathbf{x}_v^{(0)} - \mathbf{x}_w^{(0)}) \cdot (\mathbf{x}_v^{(2)} - \mathbf{x}_w^{(2)}) = -1$ , so this cap with a triple root is second-order flexible.

Furthermore, if we notice that in the flat-folded state of the tube with  $\rho = 180^\circ$ ,  $\frac{d\phi}{dz} = 0$ , the tube itself allows for a first order flex without changing the cross section angle  $\phi$ . If we attach such flat-folded state to the cap, the overall structure acquires one extra order of flexibility, and thus the structure can become third-order flexible.

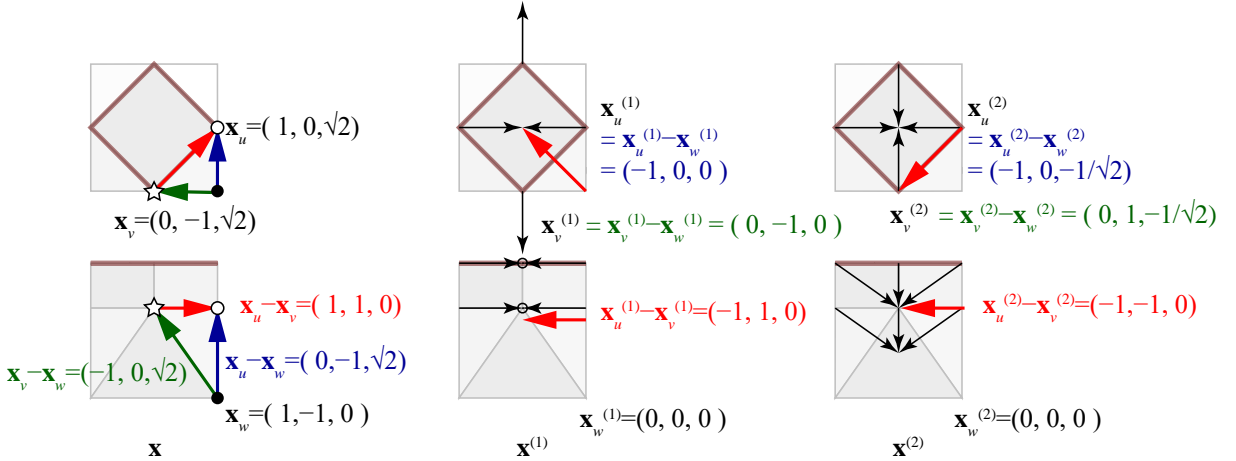


Figure 9: First order and second order flex of the cap design of Figure 5 (b).

## 5 Realization and Conclusion

Figure 10 shows a model fabricated using  $t = 0.25\text{mm}$  polyester plates glued on polyester unwoven fabric. The structure is designed to be first-order flexible at  $75^\circ$  and stable at  $45^\circ$ ; however it was impossible to feel the snap-through effect of  $e < 0.05$ .

In conclusion, we showed a parametric design for capping rigid foldable tube. By the choice of parameters, we can obtain structures from tetra-stable to third-order flexible systems that realize almost flexible capping of rigid foldable tube. By tweaking a parameter, we may also obtain a system that the deployment can be blocked at some position. We hope that this method can also effectively control the stiffness and produce a snap-through effect of the system; however, further analysis on elastic behavior

of the structure is required as our current analysis is based on partially rigid plate assumption where the stiffness may be overestimated.



Figure 10: Capped tube theoretically, infinitesimally flexible at  $75^\circ$  and stable at  $45^\circ$ .

## Acknowledgment

This work is supported by JSPS grant KAKENHI 16H06106.

## References

- [1] Z. Abel, R. Connelly, E. D. Demaine, M. Demaine, T. Hull, A. Lubiw, and T. Tachi. Rigid flattening of polyhedra with slits. In *Origami<sup>6</sup>: Proceedings of the 6th International Meeting on Origami in Science, Mathematics and Education (OSME 2014)*, volume 1, pages 109–118. 2015.
- [2] R. Bricard. Mémoire sur la théorie de l’octaèdre articulé. *J.Math.Pures Appl.*, (3):113–150, 1897. (English Translation by E. A. Coutsias: <http://www.math.unm.edu/~vageli/papers/bricard.pdf>).
- [3] R. Connelly. A flexible sphere. *The Mathematical Intelligencer*, 1(3):130–131, 1978.
- [4] R. Connelly, I. Sabitov, and A. Walz. The bellows conjecture. *Contributions to Algebra and Geometry*, 38(1):1–10, 1997.
- [5] R. Connelly and H. Servatius. Higher-order rigidity What is the proper definition? *Discrete Computational Geometry*, 11(2):193–200, 1994.
- [6] S. D. Guest and S. Pellegrino. The folding of triangulated cylinders, Part II: The folding process. *ASME Journal of Applied Mechanics*, 61:777–783, 1994.
- [7] C. Hoberman. Collapsible containers. United States Patent Application Pub.No. 2007/0007289 A1, 2007.
- [8] S. Li and K. W. Wang. Fluidic origami with embedded pressure dependent multi-stability: a plant inspired innovation. *Journal of The Royal Society Interface*, 12(111), 2015.
- [9] T. Tachi. One-DOF cylindrical deployable structures with rigid quadrilateral panels. In *Proceedings of the IASS Symposium 2009*, pages 2295–2306, 2009.